HHS Public Access

Author manuscript

Magn Reson Med. Author manuscript; available in PMC 2020 February 01.

Published in final edited form as:

Magn Reson Med. 2019 February ; 81(2): 795–802. doi:10.1002/mrm.27482.

3D High-Resolution Imaging of 2-Hydroxyglutarate in Glioma Patients using DRAG-EPSI at 3T In Vivo

Mr. Zhongxu An[1], **Vivek Tiwari**[1], **Jeannie Baxter**[1], **Michael Levy**[2], **Kimmo J. Hatanpaa**[3], **Edward Pan**[2,4,5], **Elizabeth A. Maher**[4,5,6,7], **Toral R. Patel**[2,4], **Bruce E. Mickey**[2,5,7], and **Changho Choi**[1,5,8,*]

[1]Advanced Imaging Research Center, University of Texas Southwestern Medical Center, Dallas, Texas, USA

[2]Department of Neurological Surgery, University of Texas Southwestern Medical Center, Dallas, Texas, USA

[3]Department of Pathology, University of Texas Southwestern Medical Center, Dallas, Texas, USA

[4]Department of Neurology and Neurotherapeutics, University of Texas Southwestern Medical Center, Dallas, Texas, USA

[5]Harold C. Simmons Cancer Center, University of Texas Southwestern Medical Center, Dallas, Texas, USA

[6]Department of Internal Medicine, University of Texas Southwestern Medical Center, Dallas, Texas, USA

[7]Annette Strauss Center for Neuro-Oncology, University of Texas Southwestern Medical Center, Dallas, Texas, USA

[8]Department of Radiology, University of Texas Southwestern Medical Center, Dallas, Texas, USA

Abstract

Purpose: To develop 3D high-resolution imaging of 2-hydroxyglutarate (2HG) at 3T in vivo.

Methods: Echo-planar spectroscopic imaging with dual-readout alternated-gradients (DRAG-EPSI), which was recently reported for 2D imaging of 2HG at 7T, was tested for 3D imaging of 2HG at 3T. The frequency drifts and acoustic noise induced by DRAG-EPSI were investigated in comparison with conventional EPSI. Four patients with IDH-mutant gliomas were enrolled for 3D imaging of 2HG and other metabolites. A previously-reported 2HG-tailored TE 97ms PRESS sequence preceded the DRAG-EPSI readout gradients. Unsuppressed water, acquired with EPSI, was used as reference for multi-channel combination, eddy-current compensation, and metabolite quantification. Spectral fitting was conducted with the LCModel using in-house basis sets.

Results: With gradient strength of 4 mT/m and slew rate of 20 mT/m/ms, DRAG-EPSI produced frequency drifts smaller by 5.5 fold and acoustic noise lower by 25 dB compared to conventional EPSI. In a 19-min scan, 3D DRAG-EPSI provided images of 2HG with precision (CRLB<10%) at

*Correspondence to: Changho Choi, PhD, Advanced Imaging Research Center, University of Texas Southwestern Medical Center, 5323 Harry Hines Blvd., Dallas, Texas 75390-8542, changho.choi@utsouthwestern.edu.

a resolution of 10×10×10 mm^3 for a field of view of 240×180×80 mm^3. 2HG was estimated to be 5 mM in a pre-treatment patient. In three post-surgery patients, 2HG estimates were 3 – 6 mM, and the 2HG distribution was different from the water-T_2 image pattern or highly concentrated in the post-contrast enhancing region.

Conclusion: Together with 2HG-optimized PRESS, DRAG-EPSI provides an effective tool for reliable 3D high-resolution imaging of 2HG at 3T in vivo.

Keywords

2-Hydroxyglutarate (2HG); ^{1}H MRS; 3T; Echo-planar spectroscopy imaging (EPSI); Human brain tumor; Glioma; Dual-readout alternated-gradients EPSI (DRAG-EPSI)

INTRODUCTION

The identification of 2-hydroxyglutarate (2HG) by ^{1}H MRS in patients with isocitrate dehydrogenase (IDH) mutant gliomas is a major breakthrough in neuro-oncology imaging. 2HG is the first imaging biomarker that is specific to a genetic mutation in gliomas (1), making the diagnosis of IDH mutant gliomas possible without surgery. 2HG also has a significant predictive value with respect to the stage and survival in gliomas because IDH mutation carries a favorable prognosis (2,3). Gliomas are highly heterogeneous and infiltrative. Their clinical course is characterized by progression to a higher histological grade and recurrence beyond the borders of the initial tumor mass. The need of a surveillance technique for use in extended areas of the tumor is a high priority. The tumor cellularity and the IDH activity may vary within a tumor mass, thus the spatial distribution of 2HG level may be non-uniform. A 3D imaging platform to measure 2HG rapidly is an outstanding strength for monitoring IDH-mutant tumors. With the ability to detect 2HG by high-resolution 3D MRS imaging, this metabolite could be used to follow patients with much greater accuracy.

While several single-voxel MRS methods were proposed for in-vivo detection of 2HG in patients at 3T (4–6) and the methods are translated into many hospitals and used for patient care, multi-voxel MRS imaging of 2HG, in particular 3D high-resolution imaging, remains as a challenge. In 2012, Choi et al. presented 2HG mapping in a glioma patient using phase-encoded CSI (4). Although this prior study showed that 2HG can be imaged at clinically acceptable resolution (voxel size 10×10×15 mm^3) with similar detectability as in single-voxel MRS, the application was limited to 2D imaging since 3D imaging by CSI modality is not practically feasible due to its long scan time. Recently, Andronesi et al. reported 3D imaging of 2HG using a spiral spectroscopic imaging technique combined with J-difference editing (7,8). The resolution was relatively low (voxel size 20×20×20 mm^3). The image data processing could be complicated with need of much efforts for off-resonance correction for spiral reconstruction (9) and additionally estimation of the 2HG target resonance (4.0 ppm), which is close to the water resonance, may be susceptible to subtraction errors when water suppression is suboptimal.

Recently, we reported a new MRS imaging scheme, dubbed DRAG-EPSI (echo-planar spectroscopic imaging with dual-readout alternated gradients) (10). In this prior study, the

method was used for 2D imaging of 2HG at 7T, with in-plane resolution of 6×6 mm^2. In DRAG-EPSI, the time-domain MRS signals are constructed with combined analysis of data obtained with two sets of bipolar echo-planar readout gradients. Compared to conventional EPSI, the dwell time of DRAG-EPSI is smaller by 50% for identical readout-gradient strengths, providing a twofold increase in spectral width, as shown in the 7T study. At 3T, at which the spectral width of conventional EPSI may be large enough for covering the spectral region of interest, DRAG-EPSI can be utilized for similar-quality imaging using reduced readout-gradient strengths. This may alleviate frequency drifts and acoustic noise and possibly improves the data quality and subject compliance. When compared to CSI, the benefit of EPSI may be fully realized when metabolites are imaged for large data matrix size (e.g., 3D imaging). In the present study, we demonstrate the fidelity of DRAG-EPSI for 3D high-resolution imaging of 2HG and other brain metabolites using patient-friendly readout-gradient strengths.

METHODS

MR experiments were carried out in a human whole-body 3T MR scanner (Philips Medical Systems, Best, The Netherlands) using a whole-body quadrature transmit coil and a 32-channel receive head coil (Nova Medical, Wilmington, MA). The gradient system offered maximum amplitude of 40 mT/m, with maximum slew rate of 200 mT/m/ms. In-vitro EPSI experiments were performed in a 17-cm diameter GE Braino phantom to assess the frequency drifts and acoustic noise induced by the readout gradients.

Four glioma patients were enrolled, who included an IDH1-mutated grade-II oligoastrocytoma (26-year old female), an IDH1-mutated grade-II oligodendroglioma (43-year old male), an IDH1-mutated grade-III astrocytoma (38-year old male), and an IDH2-mutated grade-IV glioblastoma (31-year-old male). The protocol was approved by the Institutional Review Board of the University of Texas Southwestern Medical Center. Written informed consent was obtained from subjects prior to MR scans.

3D DRAG-EPSI was preceded by prescription of a volume of interest (VOI) using a previously-reported 3T 2HG-optimized TE 97ms PRESS sequence (4). The PRESS sequence included a 5.8 ms 73° excitation RF pulse (bandwidth 2.5 kHz) and two 13.2 ms 180° RF pulses (bandwidth 1.3 kHz) at B_1 of 13.5 μT. The echo-planar readout gradient consisted of 1024 alternating trapezoidal gradients with amplitude of 4 mT/m and slope of 20 mT/m/ms (slope length of 200 μs and plateau length of 563 μs). Two sets of data were acquired with opposed-polarity readouts in an interleaved fashion (see Figure 1B for gradient strength and slew rate). The spectral width of the DRAG-EPSI was 1037 Hz (8.1 ppm at 3T). Imaging along two other directions was achieved with phase-encoding gradients. Water suppression was obtained with a vendor-supplied various flip angle pulse scheme that consisted of four pairs of partial-inversion and dephasing gradients (MOIST). Up to second order B_0 shimming was carried out on the VOI using a vendor-supplied tool. The scan parameters of water-suppressed 3D DRAG-EPSI included: PRESS TE 97 ms (TE_1 32 ms and TE_2 65 ms), TR 1.6 s, FOV 240×180×80 mm^2, spatial resolution 1 mL (10×10×10 mm^3), data matrix size 24×18×8×1024, number of signal averages 4, and slice-selective RF pulse carrier 2.7 ppm. The scan time was 15.36 min. Unsuppressed-water

imaging data were acquired with DRAG-EPSI and TE 97 ms PRESS and with conventional EPSI and TE 14 ms STEAM (scan times of 1.92 and 0.96 min respectively, and slice-selective RF pulse carriers at 4.68 ppm for both). All in-vivo scans were undertaken with a vendor-supplied real-time frequency drift correction tool (Frequency Stabilization), by which a reference frequency determination (~15 ms) was performed at the beginning of each TR period. T_2w-FLAIR (T_2-weighted fluid attenuated inversion recovery imaging) was acquired for tumor identification (TR/TE/TI = 9000/125/2600ms; FOV = 230×200 mm^2; slice thickness = 4 mm; 45 transverse slices).

The 3D k-space data were zero filled to 48×36×16 matrix and subsequently apodized with a 3D Hamming function. The time domain data were zero filled to 2048 points and apodized with a 2 Hz exponential function. Eddy-current compensation and multi-channel combination were conducted using the unsuppressed PRESS DRAG-EPSI water as reference, after which the two sets of interleaved data were combined without additional phase correction, similarly as in our prior study (10). Spectral fitting was performed between 1.1 and 3.7 ppm, with LCModel software, using in-house calculated basis spectra of 14 metabolites, which included 2HG, Glu, NAA, mI, Lac, Gln (glutamine), tCr (Cr + phosphocreatine), Gly (glycine), GSH (glutathione), Ace (acetate), Asp (aspartate), sI (scyllo-inositol), NAAG (N-acetylaspartylglutamate), tCho (glycerophosphorylcholine + phosphorylcholine). Since the T_2 difference between tumor and normal brain is much larger in water than in metabolites (11), the metabolite signal estimates from LCModel were normalized to the unsuppressed short-TE (14 ms) water for individual voxels, by which the data were corrected for potential B_1 variations. Subsequently the metabolite concentrations were calculated by scaling the normalized metabolite signal estimates with reference to tCr in normal-appearing gray-matter region at 8 mM (12,13). Metabolite estimates with CRLB > 20% were discarded, similarly as in prior EPSI studies (8,14,15). All data are presented as mean ± SD.

RESULTS

We compared the frequency drifts induced by DRAG-EPSI with those of conventional EPSI in a phantom solution. The spectral width was set to be similar between conventional EPSI and DRAG-EPSI (987 Hz vs. 1037 Hz). Since the spectral width in DRAG-EPSI was determined by the time interval between the adjacent odd and even number echoes, DRAG-EPSI needed much lower readout gradient strength and slew rate than conventional EPSI, as shown in Figure 1A. For each EPSI, 40 images were acquired for 20 min and subsequently the drifts of water resonance frequency were calculated with reference to the first imaging scan. The frequency drift averaged over the voxels within the phantom was much smaller (5.5 fold) in DRAG-EPSI than in conventional EPSI (7.0±1.0 vs. 38.8±1.0 Hz) (Figure 1B), which was most likely due to the differences in readout gradient strength and slew rate. With a real-time frequency-drift correction tool (Frequency Stabilization), the frequency drift in DRAG-EPSI was further reduced to 1.1±0.4 Hz (Figure 1B). Due to the difference in the readout gradient strength and slew rate, the acoustic noise of DRAG-EPSI was much less compared to conventional EPSI. When measured using a microphone placed within the receive head coil, the sound pressure level in DRAG-EPSI was 63 dB, smaller by 25 dB compared to conventional EPSI (88 dB) (Figure 1C).

The DRAG-EPSI with 2HG-tailored PRESS prescription was used for imaging of 2HG and other metabolites in four patients with IDH-mutant gliomas. For a patient with IDH1-mutant grade-II oligoastrocytoma, T_2w-FLAIR identified a solid tumor mass in the left medial-occipital region (Figure 2). In spectra from the tumor, the 2HG signal at 2.25 ppm was well discernible while the Glu 2.35 ppm signal, which was very large in spectra from the normal-appearing contralateral brain, was small. For a VOI of 100×100×65 mm^3, which included the tumor and contralateral normal-appearing brain, the maps of 2HG showed that the volume with elevated 2HG agreed well with the T_2w-FLAIR hyperintensity volume. The 2HG estimate was as high as 5 mM in the center of the tumor while normal-appearing brain showed essentially null 2HG (< 0.5 mM). tCho was substantially high in the tumor compared with normal-appearing brain regions (3.4 vs. 1.9 mM; $p < 0.001$). The tNAA and Glu levels were both decreased in the tumor. Lac was highly elevated (> 10 fold) in the tumor, indicating markedly increased glycolysis in the tumor.

Figures 3 and 4 present 3D DRAG-EPSI data from three post-surgery patients with IDH mutant gliomas. T_2w-FLAIR imaging showed lesions outside the resection cavities in all three cases. 2HG was measured to be up to 3, 6 and 6 mM in the lesions of the three patients (CRLB of 6%, 5% and 6%, respectively), indicating the lesions were all recurrent tumors. In all three cases, the tumors also showed increased tCho and Lac, as indicated in the 3D maps. For an oligodendrogliom patient (Figure 3, left), the coronal T_2w-FLAIR images showed two distinct tumor masses, among which 2HG was clearly detectable only in the lower part. In contrast, for an astrocytoma patient (Figure 3, right) who also had two distinct tumor masses, 2HG was measurable in both anterior and posterior regions of the tumor mass, as seen in the sagittal image. In a glioblastoma patient (Figure 4), the 2HG level was higher in the anterior part of the tumor mass than in other regions within the tumor, and the high-2HG regions were consistent with enhancement in T_1w post-gadolinium imaging. In all three post-surgery cases, the regions with null metabolite signals showed excellent agreement with the resection cavities indicated by T_2w-FLAIR imaging.

DISCUSSION and CONCLUSION

We demonstrate 3D high-resolution imaging of 2HG and other metabolites in brain tumor subjects at 3T, which was achieved using a newly-developed 3D DRAG-EPSI scheme together with a previously-reported 2HG-tailored TE 97 ms PRESS sequence. To our best knowledge, this is the first report of 3D imaging of 2HG with resolution of 10×10×10 mm^3, which is the same resolution as in prior EPSI studies of relatively large metabolite signals (e.g., NAA, tCr and tCho). As shown in our phantom study, the frequency drift induced by DRAG-EPSI was much smaller compared with conventional EPSI (7 vs. 39 Hz during a 20-min scan). This was most likely due to the use of relatively low gradient strengths in DRAG-EPSI given that gradient pulses cause heating in the shimming coil and consequently changes in the B_0 fields (16). It is noteworthy that in our in-vivo scans, the frequency drifts were essentially negligible (≤ 1 Hz) with the use of a vendor-supplied real-time frequency-drift correction tool, and thus our 3D imaging data may not have considerable artifacts associated with frequency drifts, obviating the need for correction of frequency instabilities which was incorporated in a prior EPSI study (16). Also, the reduction in acoustic noise in DRAG-EPSI is highly beneficial for patient scans. Brain tumor patients often show seizure

activities. The seizure incidence can be increased by extensive noise during an imaging scan. In practice, at the beginning of our development of high-resolution 2HG imaging, we were using a conventional EPSI scheme (shown in Figure 1A) and a tumor patient who was sensitive to acoustic noise developed a seizure immediately after the scan. This incident prompted us to develop a new imaging tool with much lower acoustic noise level. We believe improvement in patient comfort by reduced acoustic noise may also be helpful for minimizing potential subject movement and eventually improving the imaging data quality. In reality, the reduction of acoustic noise by 25 dB using DRAG-EPSI (Figure 1C) was greatly beneficial for 2HG imaging, as no adverse event was observed during the study and no complaint about the acoustic noise was received from the patient volunteers.

Several researchers reported imaging of 2HG in patients with IDH-mutant gliomas at 3T. In two of Choi et al. studies which used 2D phase-encoded CSI with $10\times10\times15$ mm^3 (1.5 mL) voxel size (4,17), the volumes with elevated 2HG were about the same as those with T_2w-FLAIR hyperintensity. Using a 3D spiral imaging method with $20\times20\times20$ mm^3 voxel size (8 mL), Jafari-Khouzani et al. reported larger volumes with elevated 2HG than T_2w-FLAIR volumes and partial agreement on the locations of the two volumes in more than half of the patients (7). The discrepancy in tumor volumes and locations between 2HG imaging and T_2w-FLAIR could be due to the large difference in the spatial resolution of images (8 mL vs. 0.001 mL). Published data showed great potential of 2HG imaging for monitoring disease progression (17) and treatment effects (8,17) in IDH-mutant gliomas, indicating that the 2HG level may be closely related to the clinical behavior of IDH-mutant tumors. Intermediate to high-grade gliomas are highly infiltrative. Following a gross total resection, tumors typically recur adjacent to the resection cavity. The capability to image 2HG at high resolution in 3D space can provide a tool for following IDH-mutant glioma patients with high accuracy, which was the primary goal of the present study.

DRAG-EPSI requires two excitations per k-space point at minimum. This may be acceptable for imaging of 2HG, whose signal is relatively small and may require some averaging for achieving acceptable SNR. Imaging of unsuppressed water, which is often used for eddy-current compensation, may be prolonged because of the two-excitation requirement. In the present study, the voxel size of unsuppressed-water DRAG-EPSI imaging was set to $20\times20\times10$ mm^3 (scan time 1.92 min) and the water signal of each voxel was used for correcting the eddy-current effects in 4 adjacent voxels of 2HG imaging data, similarly as in prior studies (18). We believe that the eddy-current effects were properly corrected as the effects in the four neighboring voxels were very similar. We used conventional EPSI for imaging short-TE STEAM water because of its shorter scan time (0.96 min). For whole-brain imaging, FOV may be set to be larger compared to the present study ($240\times180\times160$ mm^3 vs. $240\times180\times80$ mm^3). The increased FOV requires twofold larger number of phase-encoding gradients. One may consider changing the number of signal averages from 4 to 2, which may maintain both the 2HG imaging scan length and the SNR. The water imaging scan time may be kept acceptable by reducing the TR and/or the spatial resolution. In addition, the VOIs of the present study were relatively small ($120\times120\times65$ mm^3 or smaller) and thus may not be ideally applicable for large tumor masses. Imaging on small volumes may be practically beneficial for improving the spectral quality, which may include proper B_1 calibration and B_0 shimming, acceptable water suppression, and minimal lipid

contamination across the voxels within the VOI. We therefore chose relatively small VOIs for imaging in tumors, similarly as in several prior studies (8,19,20).

In conclusion, we demonstrate in-vivo imaging of 2HG in glioma patients using EPSI with dual bipolar readout alternated gradients (DRAG-EPSI). 3D imaging of 2HG with acquisition resolution of $10\times10\times10$ mm^3 represents a major improvement over prior 2HG imaging methods. Compared with conventional EPSI, DRAG-EPSI needs much smaller readout gradient strengths and induces much less frequency drifts and lower acoustic noise, which may contribute to higher-quality imaging of 2HG in brain tumor patients.

ACKNOWLEDGMENT

This work was supported by the National Cancer Institute of the National Institutes of Health under an award number R01CA184584 and by the Cancer Prevention Research Institute of Texas under an award number RP130427. We thank Ms. Kelley Derner and Lucy Christie for subject recruitment and Dr. Ivan Dimitrov for technical assistance.

REFERENCES

1. Dang L, White DW, Gross S, Bennett BD, Bittinger MA, Driggers EM, Fantin VR, Jang HG, Jin S, Keenan MC, Marks KM, Prins RM, Ward PS, Yen KE, Liau LM, Rabinowitz JD, Cantley LC, Thompson CB, Vander Heiden MG, Su SM. Cancer-associated IDH1 mutations produce 2-hydroxyglutarate. Nature 2009;462:739–744. [PubMed: 19935646]
2. Parsons DW, Jones S, Zhang X, Lin JC, Leary RJ, Angenendt P, Mankoo P, Carter H, Siu IM, Gallia GL, Olivi A, McLendon R, Rasheed BA, Keir S, Nikolskaya T, Nikolsky Y, Busam DA, Tekleab H, Diaz LA, Jr., Hartigan J, Smith DR, Strausberg RL, Marie SK, Shinjo SM, Yan H, Riggins GJ, Bigner DD, Karchin R, Papadopoulos N, Parmigiani G, Vogelstein B, Velculescu VE, Kinzler KW. An integrated genomic analysis of human glioblastoma multiforme. Science 2008;321:1807–1812. [PubMed: 18772396]
3. Yan H, Parsons DW, Jin G, McLendon R, Rasheed BA, Yuan W, Kos I, Batinic-Haberle I, Jones S, Riggins GJ, Friedman H, Friedman A, Reardon D, Herndon J, Kinzler KW, Velculescu VE, Vogelstein B, Bigner DD. IDH1 and IDH2 mutations in gliomas. N Engl J Med 2009;360:765–773. [PubMed: 19228619]
4. Choi C, Ganji SK, DeBerardinis RJ, Hatanpaa KJ, Rakheja D, Kovacs Z, Yang XL, Mashimo T, Raisanen JM, Marin-Valencia I, Pascual JM, Madden CJ, Mickey BE, Malloy CR, Bachoo RM, Maher EA. 2-Hydroxyglutarate detection by magnetic resonance spectroscopy in IDH-mutated patients with gliomas. Nat Med 2012;18:624–629. [PubMed: 22281806]
5. Andronesi OC, Kim GS, Gerstner E, Batchelor T, Tzika AA, Fantin VR, Vander Heiden MG, Sorensen AG. Detection of 2-hydroxyglutarate in IDH-mutated glioma patients by in vivo spectral-editing and 2D correlation magnetic resonance spectroscopy. Sci Transl Med 2012;4:116ra114.
6. An Z, Ganji SK, Tiwari V, Pinho MC, Patel T, Barnett S, Pan E, Mickey BE, Maher EA, Choi C. Detection of 2-hydroxyglutarate in brain tumors by triple-refocusing MR spectroscopy at 3T in vivo. Magn Reson Med 2017;78:40–48. [PubMed: 27454352]
7. Jafari-Khouzani K, Loebel F, Bogner W, Rapalino O, Gonzalez GR, Gerstner E, Chi AS, Batchelor TT, Rosen BR, Unkelbach J, Shih HA, Cahill DP, Andronesi OC. Volumetric relationship between 2-hydroxyglutarate and FLAIR hyperintensity has potential implications for radiotherapy planning of mutant IDH glioma patients. Neuro Oncol 2016;18:1569–1578. [PubMed: 27382115]
8. Andronesi OC, Loebel F, Bogner W, Marjańska M, Vander Heiden MG, Iafrate AJ, Dietrich J, Batchelor TT, Gerstner ER, Kaelin WG, Chi AS, Rosen BR, Cahill DP. Treatment Response Assessment in IDH-Mutant Glioma Patients by Noninvasive 3D Functional Spectroscopic Mapping of 2-Hydroxyglutarate. Clinical Cancer Research 2016;22:1632–1641. [PubMed: 26534967]
9. Posse S, Otazo R, Dager SR, Alger J. MR spectroscopic imaging: principles and recent advances. J Magn Reson Imaging 2013;37:1301–1325. [PubMed: 23188775]

10. An Z, Tiwari V, Ganji SK, Baxter J, Levy M, Pinho MC, Pan E, Maher EA, Patel TR, Mickey BE, Choi C. Echo-planar spectroscopic imaging with dual-readout alternated gradients (DRAG-EPSI) at 7 T: Application for 2-hydroxyglutarate imaging in glioma patients. Magn Reson Med 2018;79:1851–1861. [PubMed: 28833542]
11. Madan A, Ganji SK, An Z, Choe KS, Pinho MC, Bachoo RM, Maher EM, Choi C. Proton T_2 measurement and quantification of lactate in brain tumors by MRS at 3 Tesla in vivo. Magn Reson Med 2015;73:2094–2099. [PubMed: 25046359]
12. Tkac I, Oz G, Adriany G, Ugurbil K, Gruetter R. In vivo ^{1}H NMR spectroscopy of the human brain at high magnetic fields: metabolite quantification at 4T vs. 7T. Magn Reson Med 2009;62:868–879. [PubMed: 19591201]
13. Mekle R, Mlynarik V, Gambarota G, Hergt M, Krueger G, Gruetter R. MR spectroscopy of the human brain with enhanced signal intensity at ultrashort echo times on a clinical platform at 3T and 7T. Magn Reson Med 2009;61:1279–1285. [PubMed: 19319893]
14. Posse S, Otazo R, Caprihan A, Bustillo J, Chen H, Henry PG, Marjanska M, Gasparovic C, Zuo C, Magnotta V, Mueller B, Mullins P, Renshaw P, Ugurbil K, Lim KO, Alger JR. Proton echo-planar spectroscopic imaging of J-coupled resonances in human brain at 3 and 4 Tesla. Magn Reson Med 2007;58:236–244. [PubMed: 17610279]
15. Li Y, Larson P, Chen AP, Lupo JM, Ozhinsky E, Kelley D, Chang SM, Nelson SJ. Short-echo three-dimensional H-1 MR spectroscopic imaging of patients with glioma at 7 Tesla for characterization of differences in metabolite levels. J Magn Reson Imaging 2015;41:1332–1341. [PubMed: 24935758]
16. Ebel A, Maudsley AA. Detection and correction of frequency instabilities for volumetric ^{1}H echo-planar spectroscopic imaging. Magn Reson Med 2005;53:465–469. [PubMed: 15678549]
17. Choi C, Raisanen JM, Ganji SK, Zhang S, McNeil SS, An Z, Madan A, Hatanpaa KJ, Vemireddy V, Sheppard CA, Oliver D, Hulsey KM, Tiwari V, Mashimo T, Battiste J, Barnett S, Madden CJ, Patel TR, Pan E, Malloy CR, Mickey BE, Bachoo RM, Maher EA. Prospective Longitudinal Analysis of 2-Hydroxyglutarate Magnetic Resonance Spectroscopy Identifies Broad Clinical Utility for the Management of Patients With IDH-Mutant Glioma. J Clin Oncol 2016;34:4030–4039. [PubMed: 28248126]
18. Ebel A, Maudsley AA. Improved spectral quality for 3D MR spectroscopic imaging using a high spatial resolution acquisition strategy. Magn Reson Imaging 2003;21:113–120. [PubMed: 12670597]
19. Zierhut ML, Ozturk-Isik E, Chen AP, Park I, Vigneron DB, Nelson SJ. ^{1}H spectroscopic imaging of human brain at 3 Tesla: comparison of fast three-dimensional magnetic resonance spectroscopic imaging techniques. J Magn Reson Imaging 2009;30:473–480. [PubMed: 19711396]
20. Nelson SJ, Li Y, Lupo JM, Olson M, Crane JC, Molinaro A, Roy R, Clarke J, Butowski N, Prados M, Cha S, Chang SM. Serial analysis of 3D H-1 MRSI for patients with newly diagnosed GBM treated with combination therapy that includes bevacizumab. J Neuro-Oncol 2016;130:171–179.

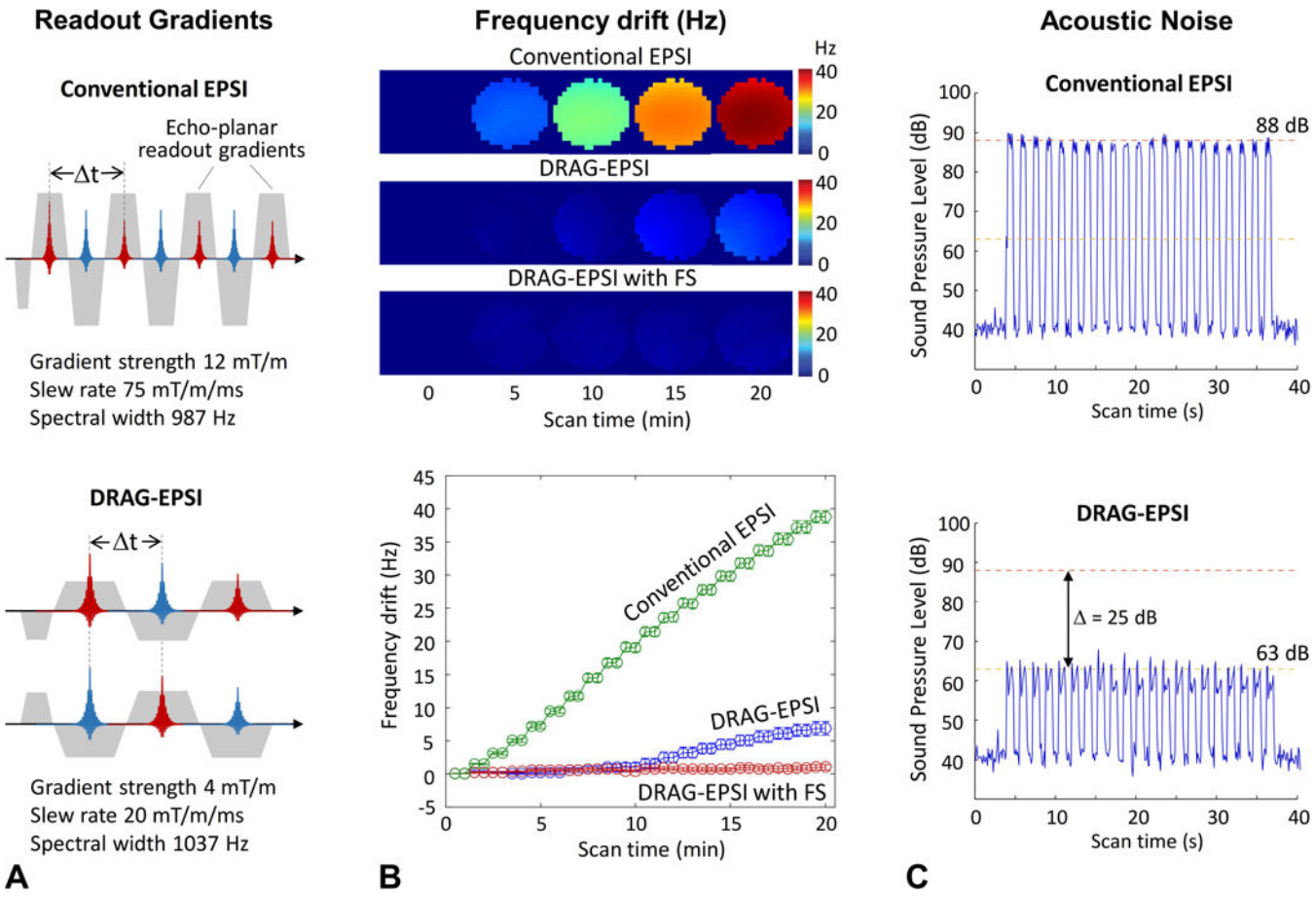

Figure 1.

A) The readout gradient schemes of conventional EPSI and DRAG-EPSI are depicted for spectral width (= 1/Δt) of 987 and 1037 Hz, respectively. **B**) Maps of Frequency drifts induced by conventional EPSI, DRAG-EPSI, and DRAG-EPSI with Frequency Stabilization (FS). Here FS denotes a vendor-supplied real-time frequency-drift correction tool. For each of the EPSI methods, 2D water imaging was undertaken for 20 min in a GE braino phantom and the water resonance frequency drifts are presented in terms of (top) frequency maps at 5 time points and (bottom) average frequency values in 40 individual images over 20 min (each imaging duration of 0.5 min). **C**) The sound pressure level, which was measured with a microphone placed inside the magnet, is shown for conventional EPSI and DRAG-EPSI.

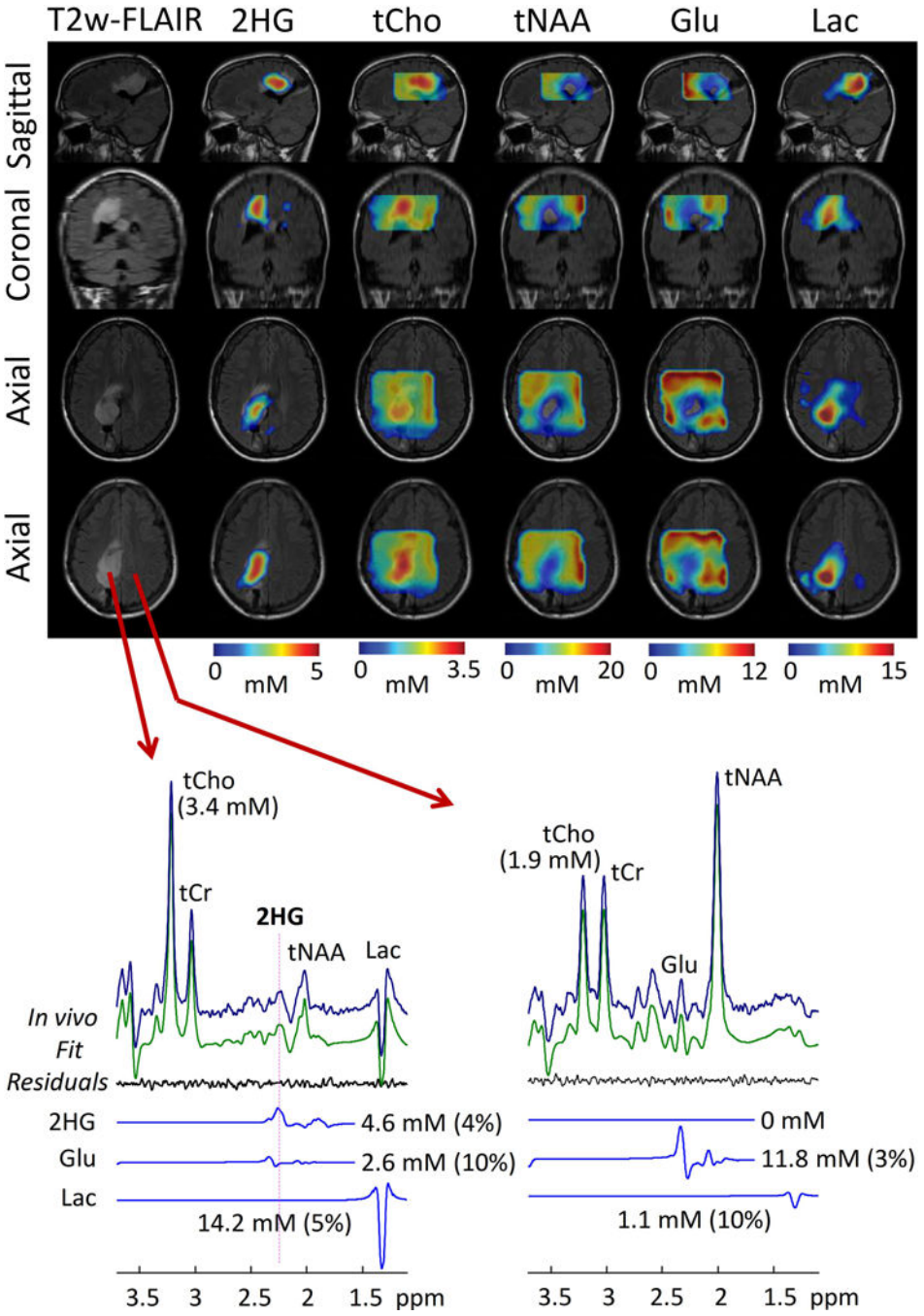

Figure 2.

In-vivo 3D DRAG-EPSI in a pre-surgery patient with IDH1-mutant glioma (Grade II oligoastrocytoma). Maps of 2HG and four other metabolites are shown on top of axial, coronal and sagittal T_2w-FLAIR images. In lower panel, representative spectra from tumor and normal-appearing regions (left and right, respectively) are shown together with LCModel outputs. A 100×100×65 mm^3 VOI (yellow box) was prescribed with TE 97 ms PRESS.

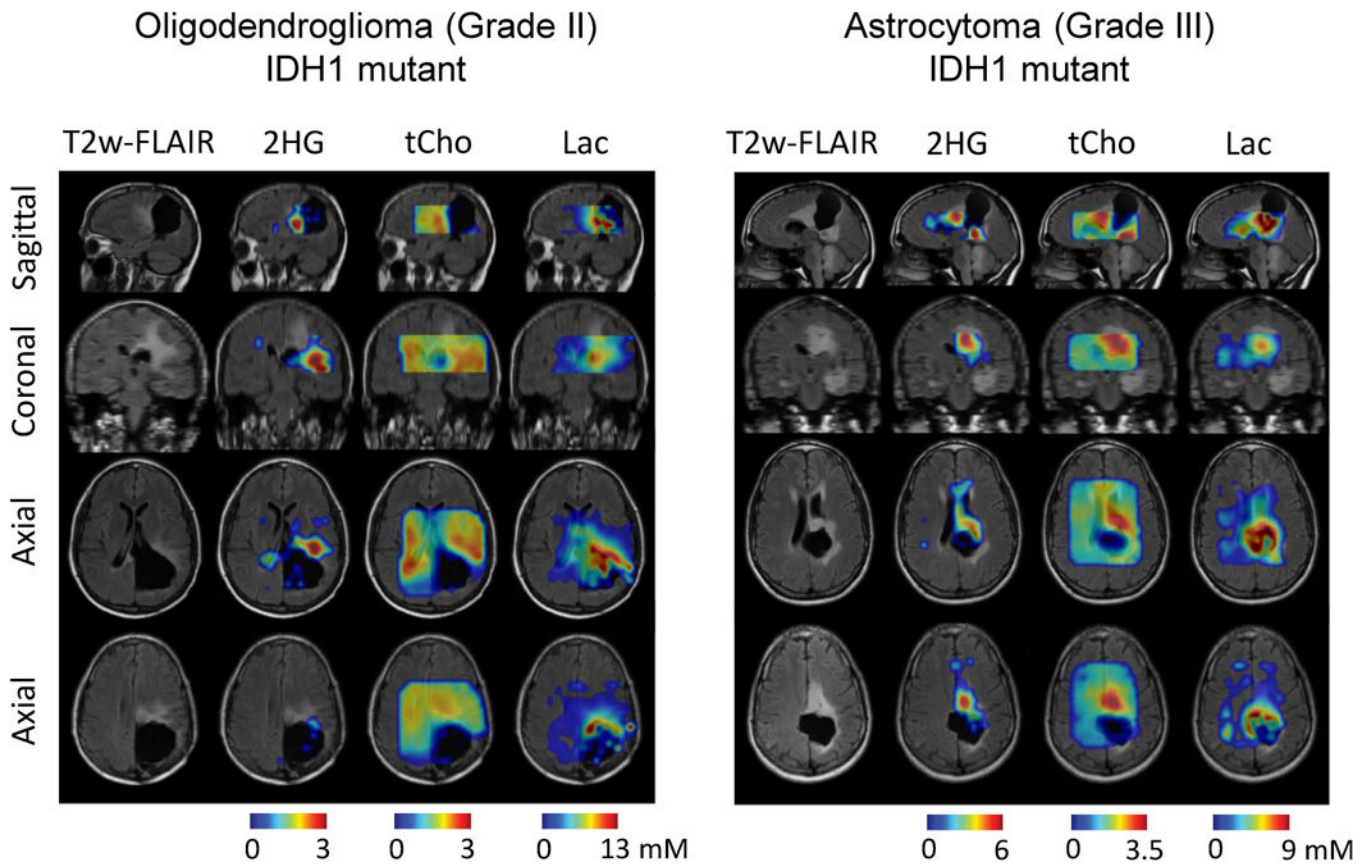

Figure 3.

In-vivo 3D DRAG-EPSI data from two post-surgery patients with IDH-mutant gliomas. Maps of 2HG, tCho, and Lac are shown on top of the axial, coronal and sagittal T_2w-FLAIR images. Tumor types and grades are displayed for each patient. VOI was prescribed with TE 97 ms PRESS.

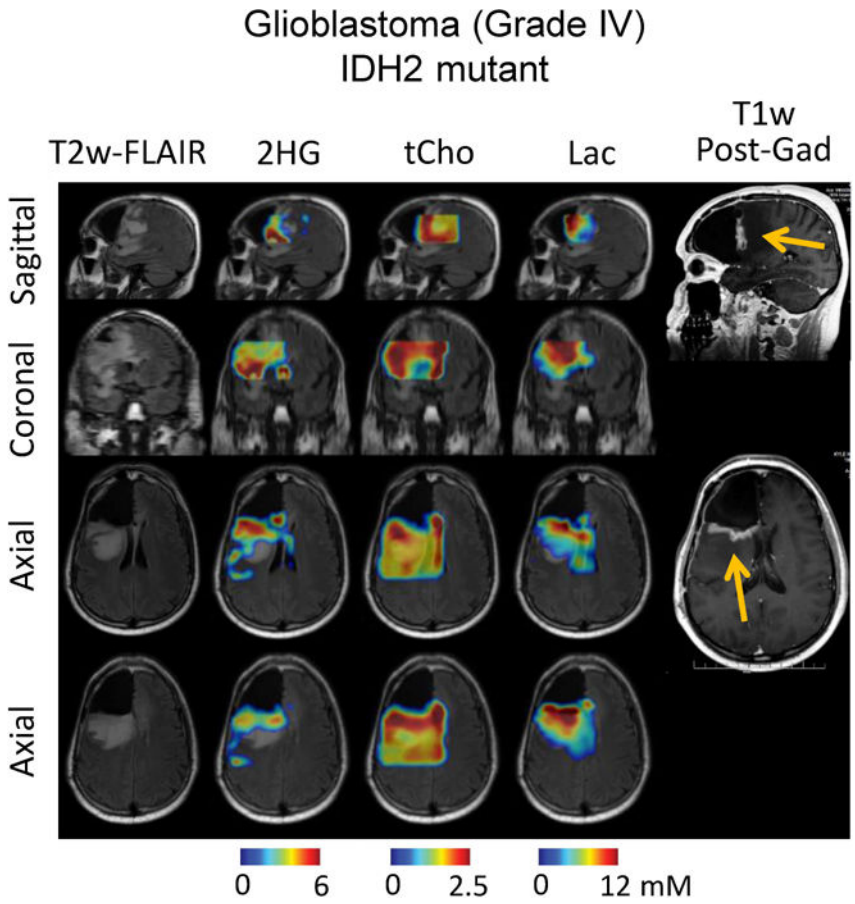

Figure 4.

In-vivo 3D DRAG-EPSI data from a post-surgery glioblastoma patient are presented in a similar fashion as in Figure 3. T_1-weighted post-gadolinium images are presented, with enhancement indicated by arrows.